# Development and validation of a DIY profiling float for indirect determination of salinity

Caleb Flaim[1]

cflaim@uw.edu

[1]University of Washington, School of Oceanography

08 March 2024

**Key words:** profiling float, low-cost, salinity, Seaglider
**Running header:** Salinity determination from buoyancy-driven devices

**Abstract**

Ocean salinity, a measure of salt concentration in seawater, is a key variable influencing water density and controls important processes like mixing and stratification. Temporal and spatial salinity variability is high in dynamic coastal systems like Puget Sound where salinity can range annually from 22 to 32 PSU. This variability occurs over small spatial scales and presents a challenge for obtaining high resolution salinity measurements. Salinity is typically measured using conductivity cells, a sensor that quantifies electrical current through seawater. These sensors can be deployed on ship-based CTDs, spatially-limited moorings, or costly AUVs, but can have limited long-term stability due to sensor drift and biofouling. This project assessed the possibility of salinity calculation from buoyancy-driven vehicles, culminating in the development and validation of a cost-efficient buoyancy-driven profiling float, dubbed openFloat, for the indirect determination of salinity. The openFloat measures in situ temperature and pressure through electronic sensors and determines water density at a given depth by achieving neutral buoyancy (e.g., float density equals water density) by adjusting its volume. Salinity can be determined by way of back calculation using the equation of state of seawater using these three known parameters. This proposed method of measuring salinity was tested in situ through multiple deployments of a buoyancy-driven Seaglider in Colvos Passage, WA (Puget Sound). Salinity was determined at the deepest point in the Seaglider's dive when it achieves neutral buoyancy and salinity is not recorded due to unstable flight conditions. Using Seaglider buoyancy parameters, salinity could be estimated to ± 0.18 PSU in situ, and with the openFloat salinity could be estimated to ± 0.11 PSU in the test pool, demonstrating the proof of concept needed for a more cost-effective option like the openFloat in dynamic systems where the range in salinity is large. Salinity calculation with openFloat can enable the large-scale

production of floats to obtain the high-resolution spatial and temporal data needed to better quantify change in dynamic coastal systems.

**Plain language summary**

The amount of salt contained in seawater, salinity, determines important ocean processes. Salinity changes by location and over different time periods. Salinity changes a lot over small distances in dynamic coastal regions like Puget Sound, WA. Salinity is typically measured with high-accuracy electronic sensors that are used from ships or ocean robots. While these sensors are widely used, they can be costly and have technical limitations the longer they are deployed. This project therefore developed and validated a cost-efficient buoyancy-driven profiling float, dubbed openFloat, for cheaply measuring salinity in dynamic coastal systems where high accuracy data is not needed to observe changes. The concept was first validated by performing the salinity estimation with an industry-grade ocean robot and then by performing the estimation with the openFloat in a test tank. The estimation of salinity though the development of the openFloat would enable the large-scale production of ocean robots to observe large changes in salinity between nearby locations in dynamic coastal systems such as Puget Sound, WA, with its ± 0.11 PSU estimation capabilities.

## Introduction

Ocean salinity, a measure of salt concentration in seawater, is a key variable influencing water density and controls important processes, like mixing and stratification. For most of oceanographic history, salinity was determined by taking the ratio of dry salt to evaporated water (e.g., grams of salt per kilogram of evaporated seawater) or though Knudsen titrations (Cox, 1963). These methods require many liters of bottle samples to be analyzed at sea or stored and transported for laboratory analysis. Knudsen titrations are historically prone to error due to chemical leaching between the samples and the glass storage vessels (Cox, 1963) during long transportation periods to land-based laboratories before ship-based lab procedures were common. More recently, bottle samples to determine high accuracy salinity have been used on cruises (e.g., GO-SHIP), but these methods can be cost inefficient, as they require the use of a ship to collect bottle samples for these measurements. Alternatively, the innovation of salinity sensors that use conductivity – a measure of electrical current though a material – as a proxy for salt concentration in seawater enabled the measurement of salt concentration with circuitry. Conductivity is used as a proxy for salinity because a well-defined positive correlation exists between water conductivity and salt concentration (Cox, 1963; Woody et al., 2000).

Initial seawater conductivity sensors were benchtop instruments and could not be used in situ, requiring bottle samples to be obtained from various depths for ship-board analysis. The advent of waterproofing technologies enabled in situ conductivity measurements to be made with conductivity cells. In situ salinity measurements with conductivity cells do not require bottle samples to be obtained regularly, but can be prone to error due to sensor calibration drift over time and biofouling (Woody et al., 2000). Salinity error due to sensor drift is an important consideration, particularly in the homogeneous deep ocean where high levels of data accuracy

(within +/- 0.0003 S/m) are required to differentiate between nearly identical water parcels. Conductivity cells capable of deep ocean salinity measurements undergo extensive regularly scheduled calibration and are expensive due to their high level of data accuracy. Common methods for measuring deep ocean salinity are through the use of autonomous underwater vehicles (AUVs) such as Seagliders or Argo floats equipped with conductivity cells. The accuracy of these sensors is optimal for deep or open ocean environments that experience low variability (e.g., Hawaii: 34 – 35 PSU ) (e.g., Lukas and Santiago-Mandujano, 2008; Stammer et al., 2021). However, the level of accuracy achieved by these sensors is often not needed to quantify variations in dynamic coastal estuarine locations such as Puget Sound, WA, where temporal and spatial variability of salinity is relatively large (e.g., 20 – 33 PSU) (e.g., Moore et al., 2008; MacCready et al., 2021).

Arrays of salinity sensors offer better data resolution to characterize the spatial and temporal variability of salinity seen in dynamic coastal systems. However, high-cost sensors can be prohibitive in these ecosystems due to the need for many sensors to observe their high variability. Current shipboard and robotic salinity sampling techniques obtain high accuracy data, but are limited in that they cannot be deployed broadly to encompass a high-variability region like Puget Sound due to cost. The Argo float fleet, an array of buoyancy-driven profiling floats, achieves a similar goal on a global scale for deep ocean environments, but are not suitable for shallower coastal areas. This study sought to develop a low-cost DIY profiling float – the openFloat – capable of salinity estimation to address this need. The main requirement for the development of the openFloat was for it to be inexpensively reproducible to increase the possible spatial resolution of observations needed to characterize dynamic systems through mass production. This study built a DIY buoyancy-driven profiling float to determine salinity through

back-calculation of the TEOS-10 equation of state of seawater (McDougall et al., 2012) by inexpensively measuring temperature and pressure along with known properties of the float (e.g., density at neutral buoyancy). This concept was first tested with an industry-grade AUV called a Seaglider.

Seagliders are another type of buoyancy-driven AUV that profile the water column with similar methods to Argo floats and the proposed openFloat. They can collect data between designated GPS coordinates by flying through the water in elongated V-shaped dives. Seagliders produce thrust to propel through water by adjusting their volume to become more or less dense than the surrounding water; the sinking or floating motion of the Seaglider in combination with its wings produces forward thrust, much like an airplane. Many Seagliders do not have conductivity sensors that actively pump water through itself and rely on near-laminar flow over its outer shell to achieve quality measurements. Seagliders experience laminar flow over the outer shell during all stages of a dive cycle except for the transition between diving and climbing. Consequently, Seagliders do not measure salinity for the deepest five to ten meters of any dive. This does not prove to be an issue when Seagliders are flown in water significantly deeper than its intended maximum depth (e.g., the deep ocean). In shallower water, such as Puget Sound, Seagliders are often flown to a maximum depth of ~10 m above the seafloor. This can result in a lack of salinity data for one-tenth or more of sampled depths.

This project addressed the question: How well can salinity be estimated from buoyancy-driven vehicles using vehicle density parameters? First, the salinity back-calculation method was validated in situ by performing the same calculations with data from Seaglider SG175, then the same method was used to calculate salinity with the openFloat in a test pool. SG175 was deployed twice in Colvos Passage, WA (Puget Sound), a channel that experiences high levels of

turbulent mixing due to sills – thin areas of rapidly reduced depth – in the local bathymetry (Seim and Gregg, 1997; Ovall, 2019). Flood tides bring water into Southern Puget Sound through East Passage (the eastern edge of Vashon Island) where it is then upwelled and mixed over a sill in the Tacoma Narrows; the ebb tide then again moves water through the Tacoma Narrows and into Colvos Passage (Seim and Gregg, 1997; Ovall, 2019). The high levels of mixing around Colvos Passage cause spatial variability of salinity to be low, enabling high confidence that calculated salinity will match measured salinity. I tested the hypothesis that salinity can be estimated to an accuracy suitable for highly variable coastal environments using buoyancy-driven devices (Seaglider and openFloat) when neutrally buoyant from the TEOS-10 equation of state of seawater if in situ temperature and pressure are measured.

## Methods

### *Colvos Passage Seaglider deployments*

Seaglider SG175 was deployed in Colvos Passage, WA, on 15 December 2023 from the R/V Weelander and completed nine dives between 6:30 PST and 14:30 PST. SG175 was again deployed in Colvos Passage on 09 February 2024 and completed eight dives between 8:30 PST and 3:30 PST. The Seaglider was deployed and recovered over the side of the research vessel using the stock cradle delivered with all Seagliders. SG175 was equipped with a standard Seabird Scientific conductivity and temperature (CT) sail and Keistler pressure sensor.

The first deployment began at the southern end of Colvos Passage and ended near Blake Island, WA (Figure 1). The second deployment began near the northern end of Colvos Passage and ended north of Blake Island (Figure 1). On average, the Seaglider dove to ~90 m with dive times ranging between 30 and 60 minutes and vertical velocities set to be ±10 cm $s^{-1}$ depending on ascent or descent. Each dive covered one to two kilometers in lateral distance. This Seaglider deployments served to collect data as a proof of concept for back-calculating salinity from the known density of an AUV at neutral buoyancy (e.g., AUV density is equal to seawater density), in situ temperature, and pressure, while the openFloat was still in development. The Seaglider did not collect salinity data at apogee (the bottom of the dive path) presenting an opportunity to test the accuracy and applicability of the salinity calculation in lieu of direct sensor

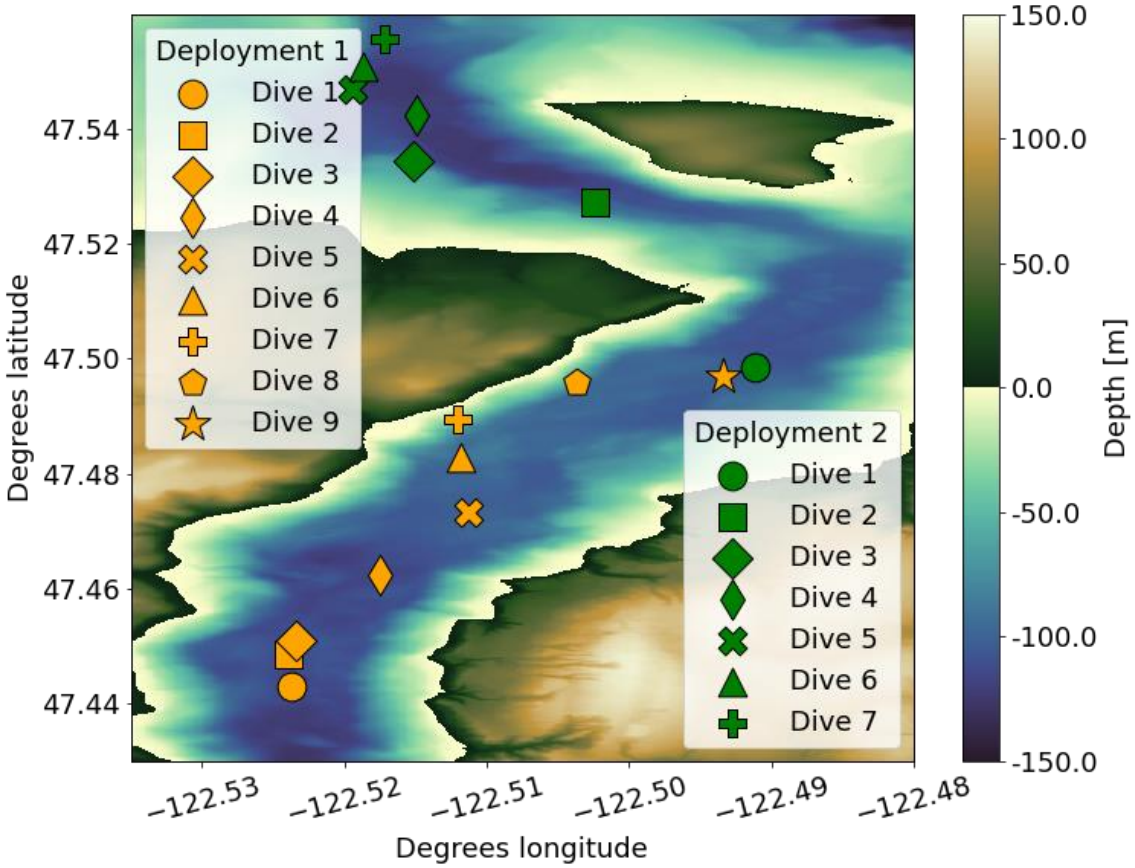


**Figure 1**. Dive locations of SG175 in Colvos Passage, WA, during the 15 December 2023 (yellow) and 9 February 2024 (green) deployments. The net northward movement is both due to planned waypoints and a northward outgoing tide.

measurements. Colvos Passage experiences high levels of mixing where water parcels throughout the channel are nearly identical, facilitating higher confidence that proof-of-concept salinity calculations would not be influenced by high environmental variability.

The salinity back-calculation was performed by feeding in situ temperature (°C) and pressure (dBar), and Seaglider density (kg $m^{-3}$) at neutral buoyancy to the Gibbs Seawater MATLAB package function named "gsw_SA_from_rho_t_exact." This function calculated absolute salinity given in situ temperature, pressure, and density. Seagliders are designed to cross neutral buoyancy during their apogee maneuver (Eriksen et al., 2001). The Seaglider's density at apogee was calculated by first isolating the base volume of the Seaglider (neglecting any added volume of the external buoyancy bladder) by subtracting the maximum volume of the buoyancy bladder from the maximum volume of the Seaglider (e.g., $V_{base} = V_{glider_{MAX}} - V_{bladder_{MAX}}$, where V is volume). This volume includes all external components of the Seaglider except for the buoyancy bladder. The volume of the buoyancy bladder at the maximum depth of apogee was then added to the Seaglider's base volume to find the Seaglider's total volume during apogee (e.g., $V_{glider_{apogee}} = V_{glider_{base}} + V_{bladder_{apogee}}$). The Seaglider's density during apogee was then computed by dividing the Seaglider's known mass by its volume at apogee.

171 ***Building the openFloat***

172 The openFloat (Figure 2) was built using
173 stock hardware, common electrical sensing,
174 and 3D-printed components. All 3D-printed
175 components were 3D printed with PETG
176 plastic using Prusa MK3s+ and Anycubic
177 Kobra2 Max 3D printers with suggested
178 print settings by the printer manufacturers.
179 Structural components, such as the motor
180 mount, were printed with 100% infill
181 density and five walls while non-structural
182 components, such as electrical board
183 mounts, were printed with 50% infill density
184 and three walls.

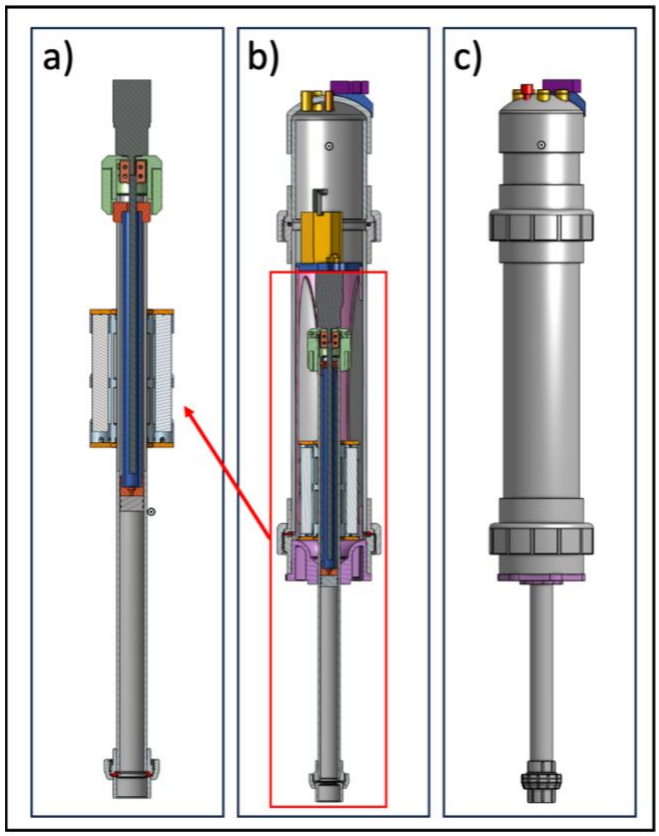


**Figure 2.** a) Isolated image of the buoyancy engine with the motor and motor mount on top, the battery pack (middle), and oil reservoir (bottom). b) Internal cross-section of the openFloat showing the internal 3D printed components (all colored components) used to hold the electrical system and operate the buoyancy piston. c) External side view of the openFloat showing the sensor cap (top), PVC pressure casing (grey components), and buoyancy engine (bottom).

185 This openFloat project was built in the
186 following five stages: electronics and sensors, variable buoyancy engine (VBE), pressure hull
187 and sensor cap, sensor and motor control code, and sensor calibration. The openFloat electronics
188 (Figure 3) are controlled by two ESP32 Feather Huzzah V2 microcontrollers paired via
189 Bluetooth. The first ESP32 (Figure 3a and b) controls all onboard sensors and writes associated
190 data to a CSV file on the internal SD card while also sending state changes to the second ESP32.

These state changes control the second ESP32 to adjust the VBE, effectively making the float move vertically through the water column. The data sensing electronics include a micro-SD card reader (Figure 3b), real-time clock (Figure 3b), electrical current meter (Figure 3c), radio for data telemetry (Figure 3d), GPS (Figure 3e), three different temperature sensors (Figure 3f), pressure (Figure 3f), and light (Figure 3f) are mounted on custom circuit boards with though-solder connections (Figure 3a). The second ESP32 (Figure 3g) controls the VBE piston position and receives movement commands over Bluetooth during state changes of the openFloat (e.g., changing from sinking to floating). The pressure (MS580305_BA) and temperature sensors (DS18b20 and built-in sensor in the MS5803) chosen for the openFloat are commonly used for DIY ocean sensors (Lyman et al., 2020; Lauer at al., 20203). The main electronics (Figure 3a-f) are stacked vertically via male-female header pins to minimize the cross-sectional area they occupy within the openFloat's pressure hull. External sensors were waterproofed and potted in the openFloat's top cap with epoxy, enabling through connections of wires from the outside of the openFloat to the main board.

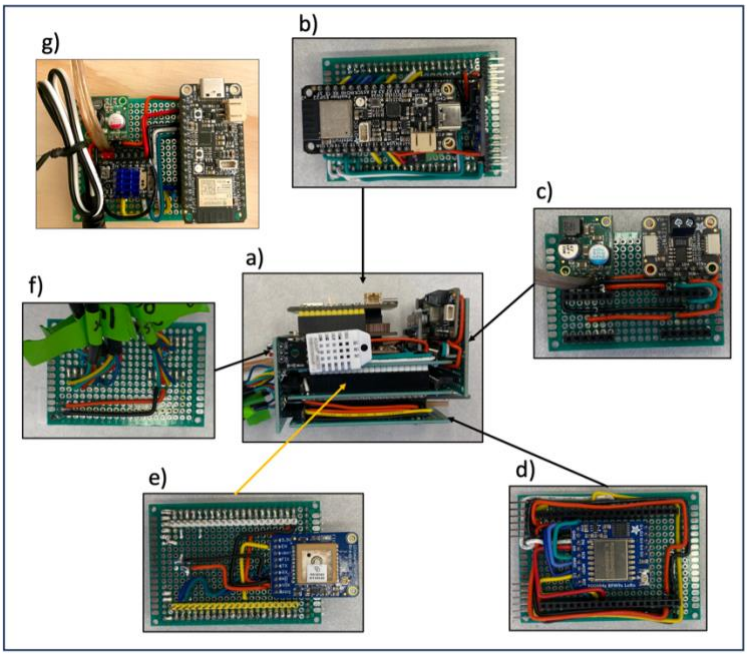


**Figure 3.** a) Side profile of the assembled electronics mainboard with all electrical connections made. b) Top view of the microcontroller board (board 1) which contains the internal pressure and temperature sensor, 3-axis accelerometer and gyroscope (compass), real-time-clock, and micro-SD card reader. c) Top view of the main power board (board 5) with a 5 V step-down converter and precision electrical current meter. d) Top view of the data telemetry board (board 3) equipped with a 915 MHz radio chip. e) Bottom view of the GPS board (board 2). f) Top view of the sensor signal distribution board (board 4) which directs signals from the external pressure, temperature, lux to the microcontroller board; this board also holds the internal humidity sensor. g) Top view of the motor control board equipped with a microcontroller and stepper motor controller.

The VBE (Figure 2a) is built from half-inch and one-inch PVC pipe, a TR8x8 ACME threaded rod, a NEMA 17 stepper motor with a 27:1 gear reduction, and 3D printed connectors. The VBE changes the openFloat's volume by actuating a piston to displace varying amounts of seawater (0 to ~250 mL). Pressure hull (Figure 2b and c) components are comprised of four-inch PVC pipe and associated connectors (see Appendix Table 1 for complete list). The main body (Figure 2c) of the pressure hull is a one-meter length of four-inch PVC with flange union connectors on either end. These flanges have built-in O-rings and enable the float to be opened to disconnect electronics, retrieve data from the on-board SD card, and remove batteries for recharging. Both the top sensor cap and bottom four-inch to one-inch connector are filled with epoxy. The top sensor cap was filled with epoxy to ensure an air-tight seal around the 3D-printed cable glands that are inserted through bore holes in the sensor cap; the bottom four-inch to one-inch connector was filled with epoxy both to lower the float's center of mass and ensure the VBE was solidly mounted. During this stage of the project, the openFloat's battery pack (Figure 4a) was also constructed. The battery pack contains sixteen 18650 Li-ion batteries (3.7 V each when fully charged) grouped in four parallel groups (Figure 4b) of four batteries in series (Figure 4c). This resultant battery is ~15 V with ~14,400

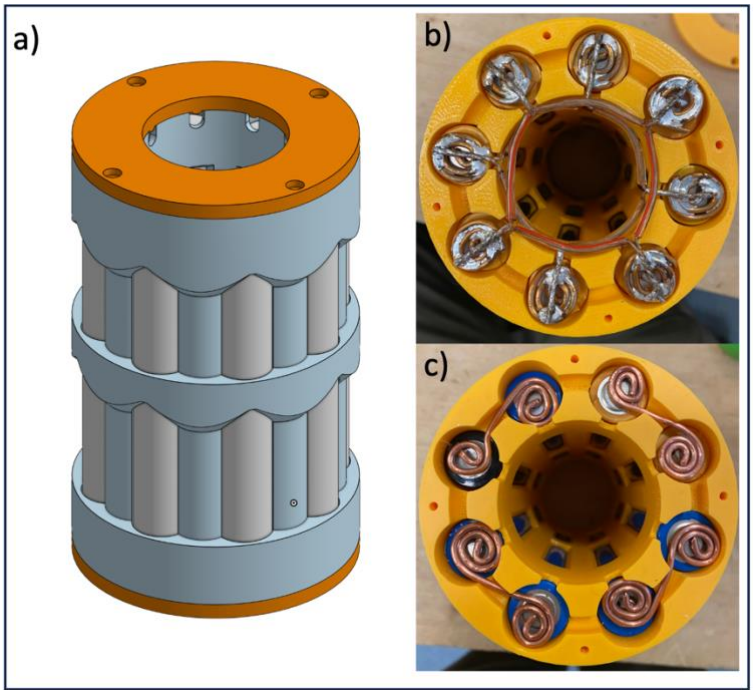


**Figure 4.** a) CAD model of the battery pack to hold sixteen 18650 batteries; blue and orange components were 3D-printed, while the grey rods represent the batteries. b) Star-patterned wiring to connect groups of four 18650 batteries in parallel. c) Wiring to connect groups of four 18650 batteries in series. b) and c) are on opposite end of the yellow 3D-printed battery pack. The battery pack is connected to the electronics through common 18 AWG speaker wire.

mAh of charge and can power the openFloat conservatively for five hours. These batteries are contained in a 3D-printed case (Figure 4a-c) and fit around the outer pipe of the VBE (Figure 2a).

All electrical components of the openFloat are programmed using the open-source Arduino IDE and make use of Adafruit, stepper motor, Bluetooth, and clock libraries (the full repository of code can be found here: https://github.com/cflaim1123/openFloat_thesis/tree/main). The openFloat runs as a state machine to control its dive cycle. State machines are blocks of computer code that have finite quantities of Boolean states that can be toggled as True or False. When specific states are True, other blocks of code are triggered to run, causing the VBE to increase buoyancy, for example. The openFloat continually runs two state machines to create the dive cycle. The first state machine tracks if the openFloat is in functioning order

**Table 1.** List of openFloat states used by its state machine operating system.

| Machine | State | Description |
|---|---|---|
| Dive cycle controller | Dive | When True, the VBE performs a bleed move where oil is removed from the external bladder, causing the float to descend. |
| | Climb | When True, the VBE performs a push move where oil is added to the external bladder, causing the float to ascend. |
| | Park | When True, the VBE maintains its position waiting for the float to become neutrally buoyant. |
| | Surface | When True, the float maximizes its volume when already at the surface to increase the antennas' height to increase chance of successful data transmission and GPS fix. |
| Force surface controller | Abort | When True, all currently True states of the float are set to False, sampling is stopped, and the VBE performs a push move to maximize the float's volume, causing it to perform an emergency surface maneuver. |
| | All clear | When True, the openFloat is safe to proceed as normal and will continue diving until its dive duration requirements are met. |

(e.g., if internal pressure or humidity changes, this state machine forces the openFloat to surface); the second state machine controls when and how much the VBE changes the openFloat's density. The main states of the openFloat and their functions are described in Table 1. The openFloat also has global parameters to determine properties such as sampling rate or deep sleep frequency that are altered by each state.

***Testing the openFloat***

The openFloat was tested in a four-meter-deep saline test tank in the Ocean Sciences Building at University of Washington Seattle campus. The openFloat was made neutrally buoyant by adding mass (~3 kg) to the pressure hull in the form of lead strips until it held position at one meter water depth. A YSI EXO Sonde CTD was then used to find the density of the test tank when the openFloat was neutrally buoyant. Since the openFloat was neutrally buoyant (e.g., float density equals tank density) and of known mass, its volume was calculated by dividing the float's mass by the test tank density (e.g., $V_{float} = \frac{M_{float}}{\rho_{tank}}$, under the assumption $\rho_{tank} = \rho_{float}$). This calculated volume was later used in salinity calculations.

Test tank salinity was determined by taking pressure and temperature readings every two seconds for five minutes from the neutrally buoyant openFloat. The openFloat was collocated with a CTD at one meter for direct measurement comparison. An offset calibration was applied to the openFloat's temperature readings by subtracting the difference in mean temperature from the float and CTD from the float's measured value (e.g., $T_{corrected} = T_{float} - avg(T_{float} - T_{CTD})$). This was done to ensure spurious salinity measurements were not made due to uncalibrated temperature measurements from the MS5803 pressure sensor. In situ pressure, corrected temperature, and calculated float density were then fed into the same MATLAB

273 "gsw_SA_from_rho_t_exact" to calculate salinity with units of g $kg^{-1}$. This value was then
274 converted to match the PSU unit used by the Seaglider and CTD using the Gibb's Seawater
275 function "SP_from_SA" to not introduce error into the comparison values. The openFloat's
276 salinity estimation was then intercalibrated with the YSI EXO Sonde CTD using the same

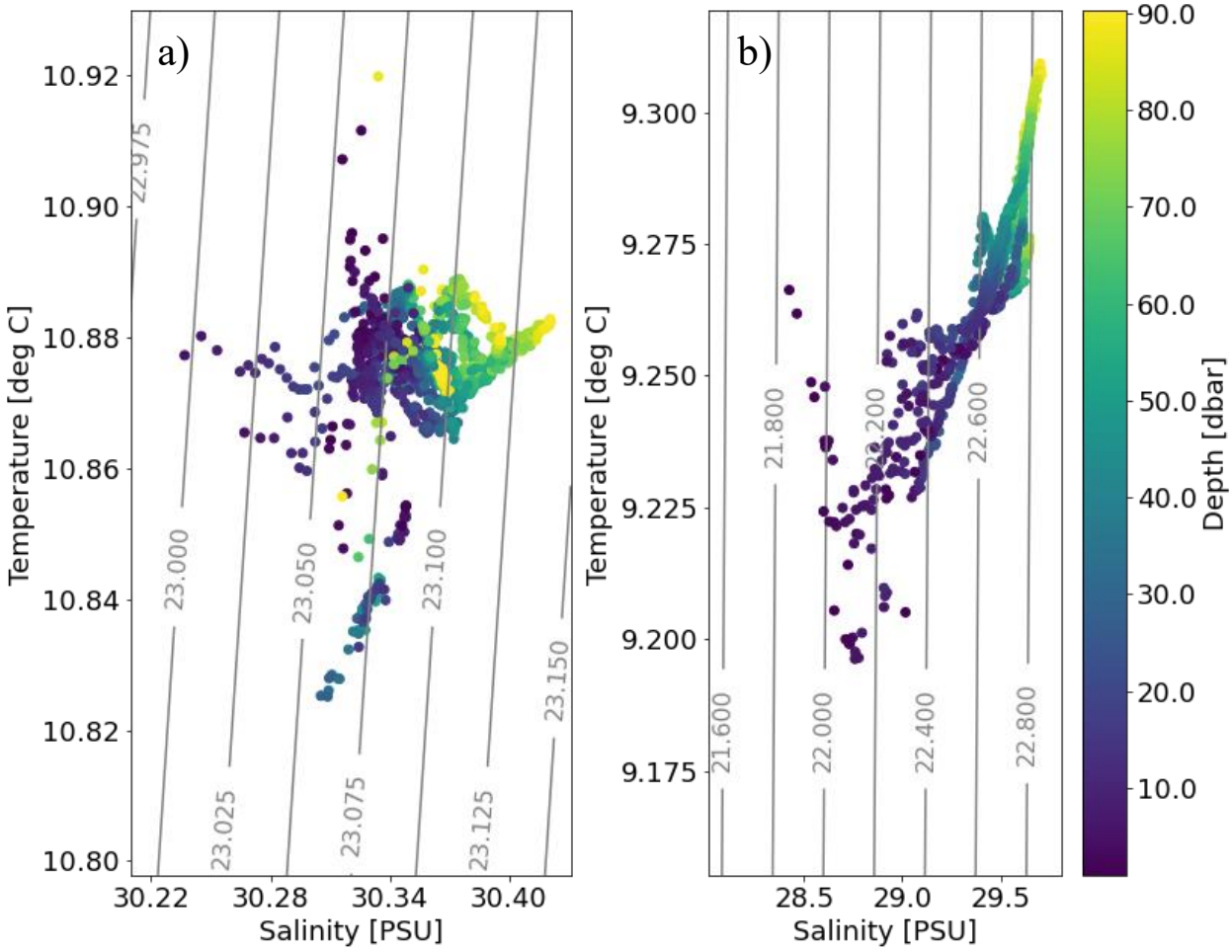


**Figure 5.** In situ Temperature plotted against salinity measured by SG175 with isopycnals super-imposed showing the clustering of density measurements during the a) 15 December 2023 Colvos passage b) 9 February 2024 Colvos passage deployments. Depth is shown as color.

277 method applied to the temperature values (e.g., $S_{corrected} = S_{float} - avg(S_{float} - S_{CTD} * k)$,
278 where $k$ is a conversion factor to account for the difference in conductivity readings between test
279 tank water and seawater) to yield corrected values.

280

## Results

The first and main result of this study is the development of the electrical and mechanical systems that yield a cost-effective DIY profiling float capable of the indirect determination of salinity. This cost of the openFloat (~600 USD) is one to three orders of magnitude cheaper than existing buoyancy-driven systems (e.g., µfloats (micro floats) (Harrison, 2021), Argo floats, Seagliders) and enables large-scale production due to reduced production cost. This study additionally found that salinity can be determined from buoyancy-driven AUVs (commercial and DIY) if they are of known mass and volume and achieve neutral buoyancy while measuring in situ temperature and pressure.

### *Seaglider salinity calculations*

Colvos Passage, WA, was well-mixed on 15 December 2023 during the first Seaglider deployment. In situ temperature and measured salinity varied between 10.87 and 10.92 °C and 30.22 and 30.40 PSU, respectively (Figure 5a). Sigma theta varied by less than 0.3 kg $m^{-3}$ during all dives (Figure 5a). Sigma theta was between 23.02 and 23.06 at the surface while sigma theta at depth was between 23.1 and 23.12. The water column was more stratified and fresher on 09 February 2024 (Figure 5b) during the second deployment enabling the salinity back-calculation test across a wider range of environmental conditions. Temperature ranged between 9.175 and

299 9.300 °C and measured salinity varied between 28 and 29.5 PSU (Figure 5b). Density varied by
300 about one sigma theta during all dives with surface sigma theta between 21.8 and 22.6 and sigma
301 theta at depth between 22.6 and 22.8 (Figure 5b). Seaglider dive depth did not exceed 100 m
302 during both deployments due to local bathymetry. The density structure of Colvos Passage
303 (Figure 6a) is well-mixed with density varying by less than 0.06 kg $m^{-3}$ over 100 m. Some dives
304 during this deployment experienced unstable water columns with less dense water sitting below
305 dense water. The western side of Blake Island (Figure 6b) was well-stratified with sigma theta

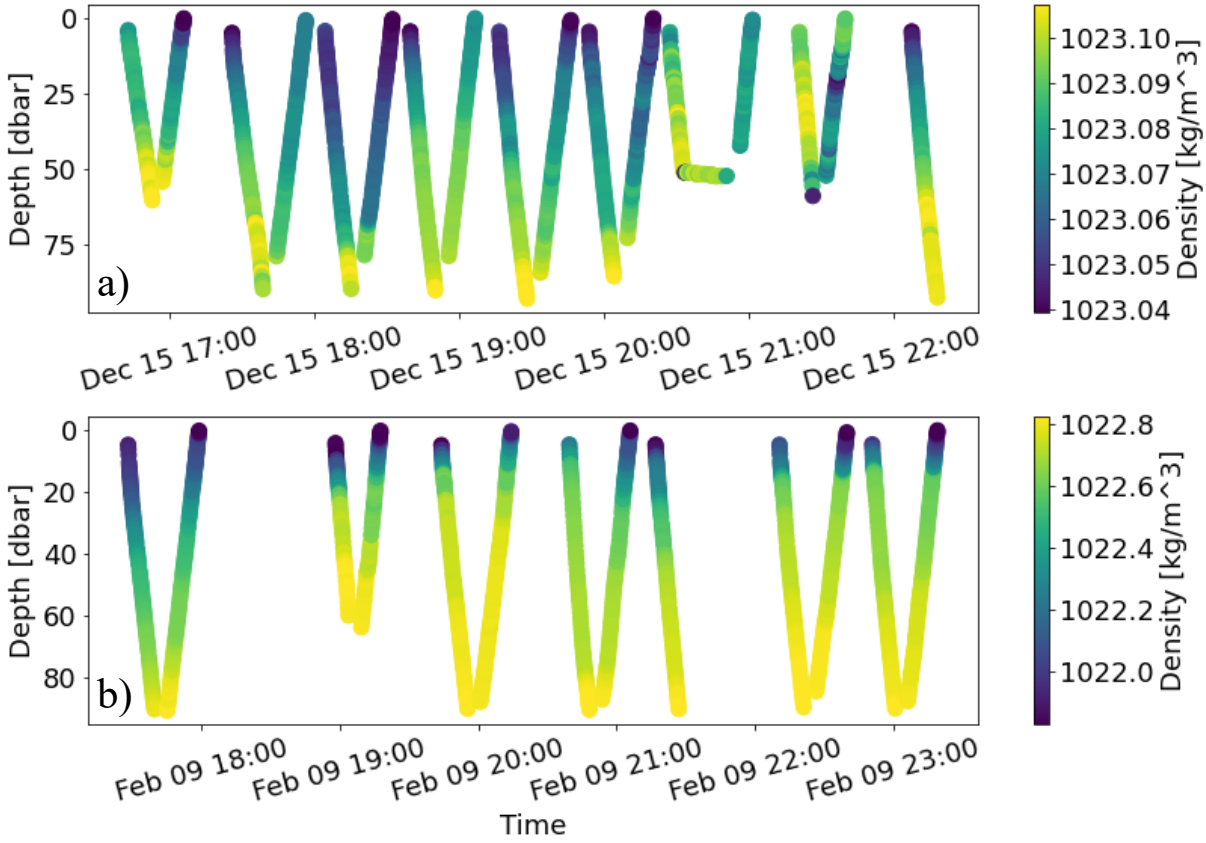


**Figure 6.** a) The dive path of SG175 during the 15 December 2023 deployment in Colvos Passage plotted as depth v.s. time with color indicating water density along the glider's path. b) The dive path of SG175 during the 09 February 2024 deployment near Blake Island plotted as depth v.s. time with color indicating water density along the glider's path.

306 varying by 0.8 kg $m^{-3}$ over 100 m. The Seaglider experienced stable water columns for all dives
307 during this deployment.

Water temperature during both dives varied by less than 0.5 °C (Figure 7). The 15 December 2023 deployment saw water temperatures between 10.87 and 10.92 °C (Figure 7a); the water column was well-mixed and does not exhibit a clear depth-dependent signal based on temperature. Southern Colvos Passage (left-hand side of Figure 7a) was warmer than the northern end (right-hand side of Figure 7a) where Colvos Passage meets the main basin of Puget Sound. The 09 February 2024 deployment of SG175 found water temperatures between 9.18 and 9.30 °C (Figure 7b). The water column was stratified with temperature increasing with depth (Figure 7b). Each dive during this deployment exhibited similar depth-dependent temperature signals.

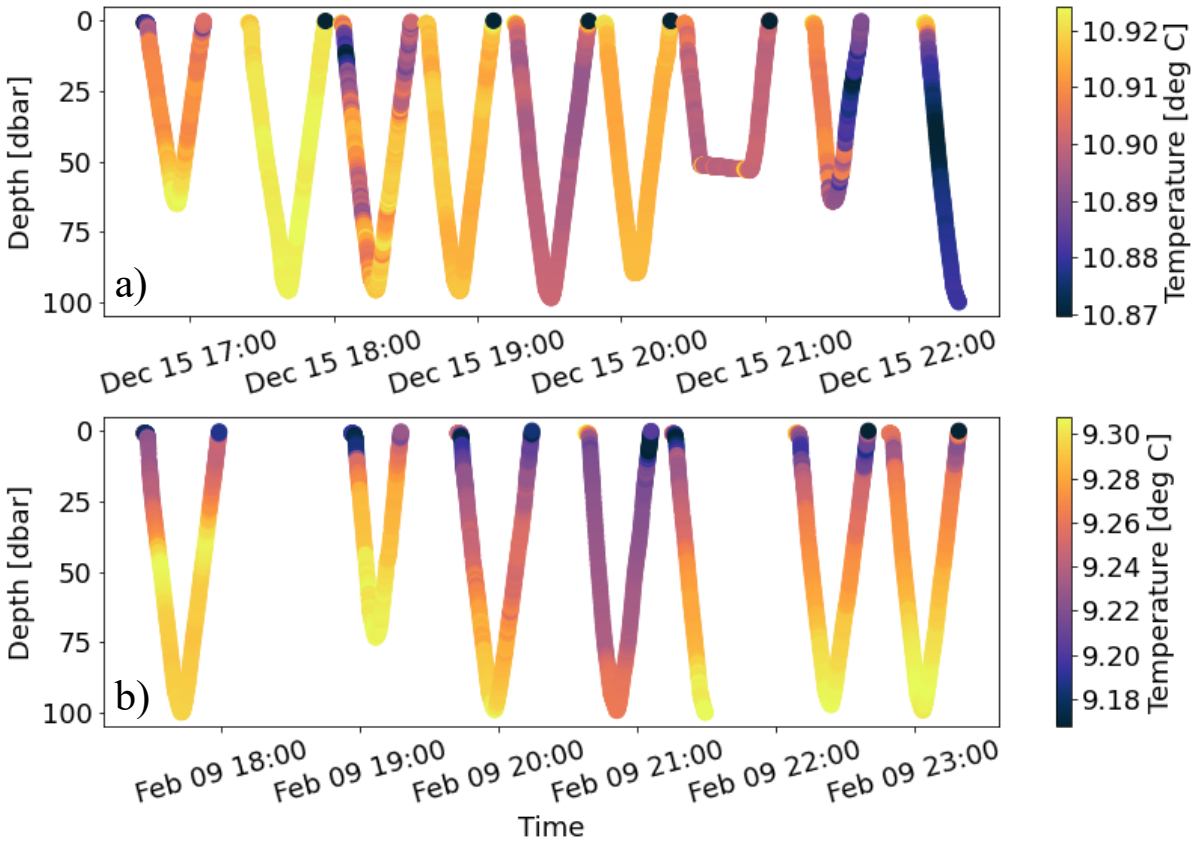


**Figure 7.** a) The dive path of SG175 during the 15 December 2023 deployment in Colvos Passage plotted as depth v.s. time with color indicating water temperature (°C) along the glider's path. b) The dive path of SG175 during the 09 February 2024 deployment near Blake Island plotted as depth v.s. time with color indicating water temperature (°C) along the glider's path.

317 Salinity in Colvos Passage varied by no more than about one PSU during both
318 deployments (Figure 8). The first deployment found salinities between 30.17 and 30.25 PSU
319 (Figure 8a). Salinity generally increased with depth. Surface salinity was between 30.18 and
320 ~30.22 PSU and salinity at depth was consistently between 30.24 and 30.25 PSU (Figure 8a).
321 The second deployment found salinities between 28.3 and 29.5 PSU (Figure 8b). Surface

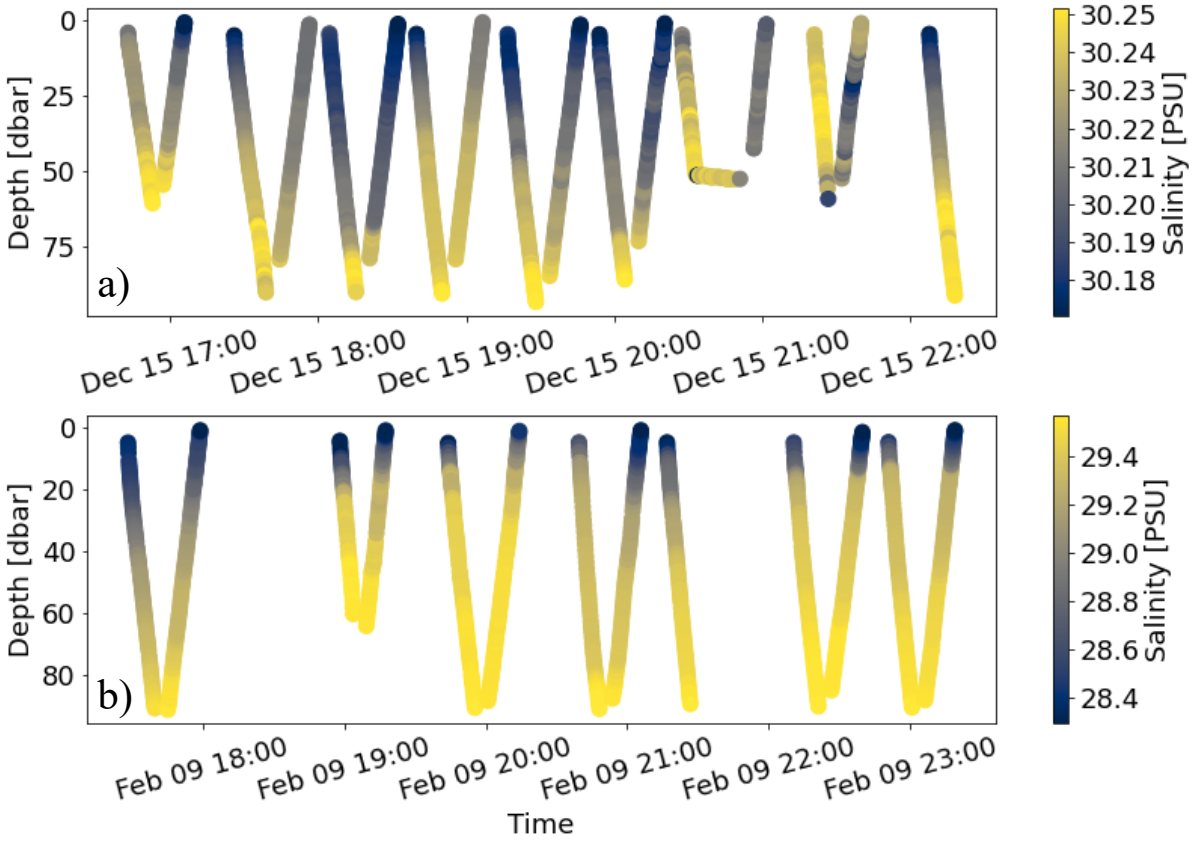


**Figure 8.** a) The dive path of SG175 during the 15 December 2023 deployment in Colvos Passage plotted as depth v.s. time with color indicating water salinity (PSU) along the glider's path. b) The dive path of SG175 during the 09 February 2024 deployment near Blake Island plotted as depth v.s. time with color indicating water salinity (PSU) along the glider's path.

322 salinities varied between 28.3 and 28.8 PSU and salinity at depth ranged between 29.2 and 29.5
323 PSU. Salinity increased with depth, causing a stratified water column.

324 Depth-averaged salinity measured by the Seaglider's conductivity cell during both
325 deployments was 30.068 PSU with a standard error of 0.093. The average calculated salinity
326 using the Seaglider's density at neutral buoyancy, in situ temperature, and pressure was 29.89

PSU with a standard error of 0.088. A T-test of the data showed the means of the two salinity measurement methods are not statistically different (t-statistic: 1.412, p-value: 0.168). This indicates no significant difference between the measured and calculated salinity values. Calculated and measured salinity at apogee from both deployments were linearly regressed and yielded a slope of 0.907, an r-squared value of 0.92, and a p-value < 0.001 (Figure 9), showing that the regression is significant. Two distinct water masses were sampled during the two deployments with salinity estimates from deployment two being more tightly grouped than from deployment one.

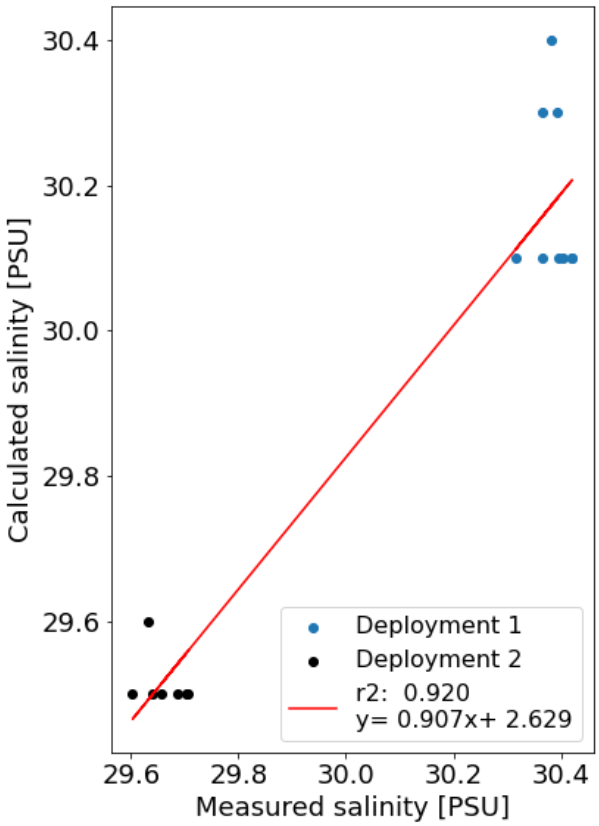


**Figure 9.** Calculated salinity using Seaglider density at neutral buoyancy during apogee plotted against the expected salinity during apogee overlayed with a linear regression. Expected salinity is calculated as the mean of salinity at the beginning and end of apogee.

***openFloat salinity calculations***

The openFloat performed similar salinity estimations in a four-meter-deep saline test tank in the Ocean Sciences Building (University of Washington). These measurements were compared to a YSI EXO Sonde CTD (Figure 10a). The YSI CTD measured tank salinity to be 33.575 ± 0.006 PSU (mean ± SD, Figure 10a) and tank temperature as 20.137 ± 0.001 °C (mean ± SD, Figure 10b). Salinity determined from the openFloat was 33.46 ± 0.01 PSU (mean ± SD, Figure 10a) upon the equilibration of its temperature sensor to 20.17 ± 0.03 °C (mean ± SD, Figure 10b) after

~100 seconds. The openFloat's salinity estimations were 0.11 ± 0.01 PSU (mean ± SD, Figure 10a) less than the salinity measured by the YSI EXO Sonde. The mean difference in temperature measured by the openFloat and YSI EXO Sonde after equilibration was 0.037 ± 0.028 °C. This analysis also showed the response time of the openFloat's temperature sensor to be approximately 100 s.

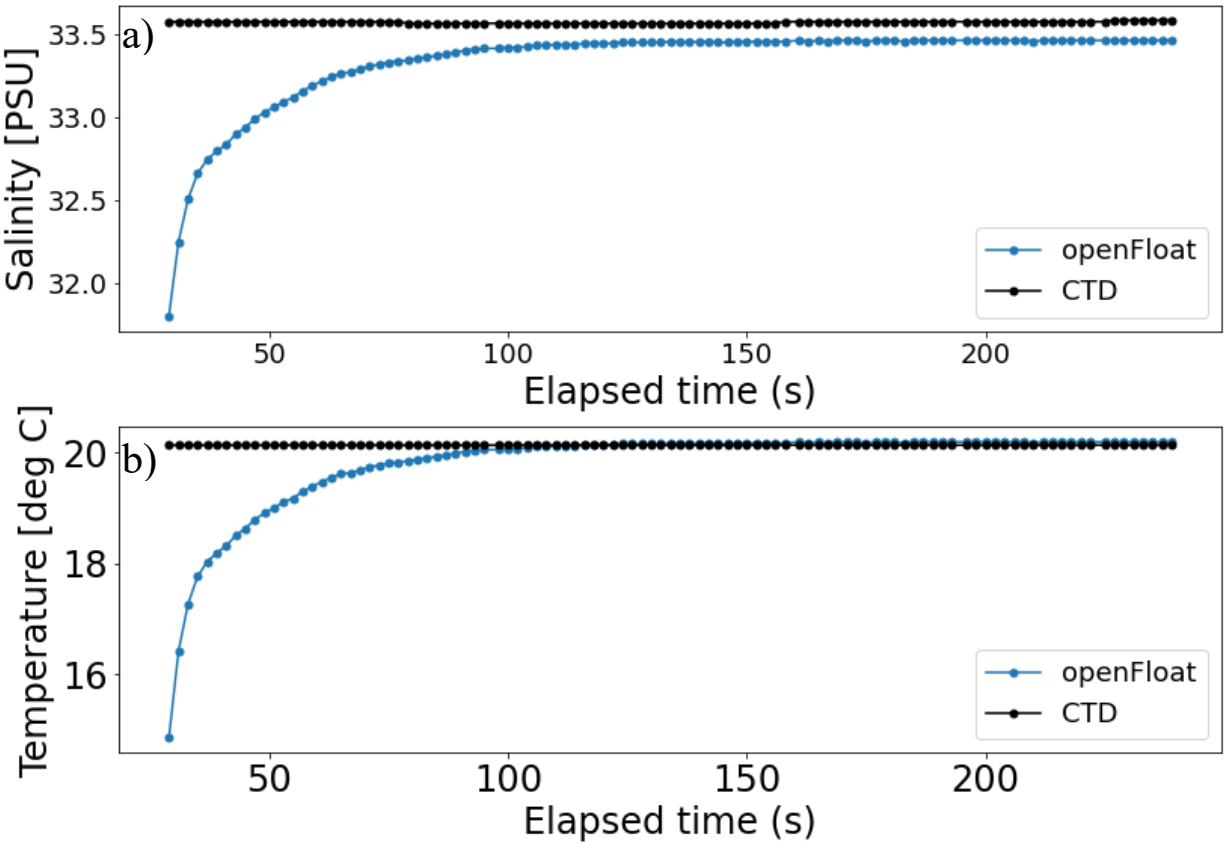


**Figure 10**. a) Test tank salinity (PSU) measurements made by a YSI EXO Sonde CTD and the openFloat through back-calculation plotted against elapsed time during sampling. b) Temperature (°C) measured by a YSI EXO Sonde CTD and the openFloat plotted against elapsed time during sampling. Temperature measured by the openFloat was inter-calibrated with the YSI to obtain accurate values.

## Discussion

### *Summary of results*

This study determined that salinity can be estimated from buoyancy-driven AUVs not equipped with a traditional conductivity cell-based sensor. Field-based salinity estimations were

performed with Seaglider SG175 in Colvos Passage, WA, during two deployments. Using SG175's in situ measured variables (e.g., temperature and pressure) and known mass and volume at apogee, salinity was measured to be 29.9 ± 0.34 PSU (mean ± SD). The mean difference between the expected salinity and the calculated salinity was 0.18 ± 0.10 PSU (mean ± SD). Likewise, the openFloat, when neutrally buoyant, estimated test tank salinity using onboard temperature and pressure readings within 0.11 ± 0.01 PSU (mean ± SD) of the true salinity as determined by a YSI EXO Sonde CTD. These accuracies are well within the range of variability in coastal Puget Sound (Babson et al., 2006; Moore et al., 2008; MacCready et al., 2021), indicating this method exhibits promise for use in these types of environments.

***Reasons that contribute to errors in calculations***

These salinity calculations are currently limited by several factors. Primarily, they are most limited by mass and volume measurements which govern calculations of AUV density. Seagliders are large and weigh roughly 50 kg; typical scales used to weigh a Seaglider are accurate to one gram. Additionally, obtaining an accurate physical measure of an AUV's volume can be challenging. Digital designs offer an idealized estimate of what the expected volume is, but this may not reflect the AUV's true volume after manufacturing. The volume of a buoyancy-driven AUV can be determined by making the AUV neutrally buoyant in a body of water with known density (e.g., a test tank). The AUV's volume can be calculated by dividing its known mass by known density; this density can be obtained with a CTD. While measuring the physical volume of an AUV is challenging, obtaining the change in volume of an AUV due to changes in its buoyancy system is known to a high level of accuracy. Both Seagliders and the openFloat use motor-controlled buoyancy systems capable of sub-100µm positional accuracy.

383 For Seagliders specially, the assumption of neutral buoyancy in the field may not be fully met
384 since the glider is never in a completely stationary position at one depth, which may influence
385 the calculation accuracy. Prior to deployment, Seagliders are ballasted and tuned to be nearly
386 neutrally buoyant at the expected maximum depth. Seagliders are not designed to maintain depth
387 at neutral buoyancy, but rather momentarily pass through neutral buoyancy as their buoyancy
388 engines begin to pump during the apogee maneuver. Since Seagliders become neutrally buoyant
389 once per dive cycle, this results in one salinity point estimation per dive. The assumption of a
390 stationary AUV at neutral buoyancy is not fully met in the salinity calculation with SG175 since
391 Seagliders never fully attain neutral buoyancy (e.g., parking at one depth). This likely limits the
392 accuracy of the salinity estimation using the Seaglider platform.
393 For the openFloat specifically, limitations of off-the-shelf sensors likely contribute to how
394 well salinity can be calculated. The pressure sensor's temperature readings have a slow response
395 time to equilibrate with environmental conditions due to the pressure sensor being potted in
396 epoxy and are limited in resolution based in the sensor's 22-bit ADC. This limits the speed at
397 which temperature readings can be made and introduces errors if salinity is calculated too
398 quickly. However, tests in the pool helped constrain the time required (100 s) for the float to park
399 in specific conditions such that a better measurement can be made once all sensors have
400 equilibrated to the environment. Because of the smaller observational resolution of the off-the-
401 shelf sensors, openFloat data may appear to have smaller standard deviations and errors than
402 industry-grade sensors.
403
404
405

406 ***Suggested use cases and benefits of the method***

407 This method presents several potential benefits. Back-calculating salinity this way does not
408 rely on traditional methods that may be prone to error due to biofouling and sensor drift, or
409 cracks in the sensors itself. This method of determining salinity can be applied in-post after an
410 AUV has been deployed for some time since back-calculating salinity does not require a physical
411 modification to an AUV; it also provides a form of redundancy if a conductivity cell does break.
412 For existing systems like Argo floats or μfloats that park at neutral buoyancy for extended
413 periods of time, this calculation can be used to create time series data rather than single-point
414 measurements that Seagliders can obtain during a dive.

415 These salinity calculations are currently limited in depth space, as they can only be
416 performed when an AUV is neutrally buoyant at the bottom of a profile or is stationary at one
417 depth. For Seagliders, this occurs briefly during the apogee maneuver as the glider passes from
418 sinking to floating; profiling floats can maintain neutral buoyancy for extended periods of time,
419 unlike Seagliders. Because this method cannot currently produce depth profiles, it may be best
420 suited for a vehicle that either follows a specific water mass at depth or one that performs a duty
421 cycle to incrementally park floats at different depths as the vehicle ascends to create a depth
422 profile. This means this method of essentially using an AUV as a density sensor when neutrally
423 buoyant is most appropriate for profiling floats over Seagliders.

424 Since profiling floats present the best use case for this method, the salinity calculations could
425 be further tested with global Argo data to expand the salinity range and add more data over
426 which to test the accuracy of the method. This also presents a way to get salinity data should a
427 conductivity cell on a float get damaged once deployed and the float becomes inaccessible to
428 retrieve.

For the DIY AUV use case, this method of calculating salinity is best used in regions with large swings in daily and annual salinity. Off-the-shelf temperature sensors are likely not accurate enough to be used in locations that experience little variation in salinity. This salinity estimation method is most appropriate for coastal systems that experience high variability, like Puget Sound, WA, that exceeds the limitations in accuracy (Babson et al., 2006; Moore et al., 2008; MacCready et al., 2021). This would not be suitable for the open ocean or deep ocean where observed changes are smaller than the current accuracy of the method (Lukas and Santiago-Mandujano, 2008; Stammer et al., 2021).

***Potential improvements to the openFloat***

Future improvements for the openFloat will likely include upgrading the custom circuit boards to printed circuit boards for ease of mass production. This electrical redesign is likely to incorporate a different microcontroller as the float's main controller in order to use the one-wire communication protocol. The ESP32 Feather Huzzah V2 is not currently able to communicate with sensors such as the ds18b20 temperature probes that are mounted on its sensor cap due to a known bug in the ESP32 V2 architecture with the one-wire communication protocol. This temperature sensor is low-cost and has an accuracy of ± 0.1 °C (Thaler et al., 2024) when readings are averaged from three sensors (currently equipped on the openFloat). Additionally, future improvements include performing the openFloat's salinity calculation in a wide range of salinities and temperatures to quantify the accuracy of its calculations in a variety of environmental conditions found in Puget Sound. Most improvements to be made are in software to increase the energy efficiency of the float as a whole.

### *Future use of the openFloat*

Future tests to validate the openFloat may include side-by-side deployments of the openFloat alongside a Seaglider for in situ data comparison to a known standard measurement. Colvos Passage, WA, poses as a unique location for such tests since the water column in nearly homogenous, ensuring that both AUVs measure similar water parcels. The production and growth of an openFloat fleet to create a low-cost array of sensors could help increase coastal observations, document change in real time and help support digital models and forecasting (e.g., the Live Ocean Model).

## Conclusions

This project developed a cost-efficient profiling float made from common and easily producible parts to indirectly measure salinity in dynamic coastal systems to increase the spatial resolution of salinity measurements. This project successfully validated the indirect determination of salinity using properties of buoyancy-driven AUVs at neutral buoyancy and sensor measurements of temperature and pressure. The indirect determination of salinity was evaluated using both a Seaglider and a DIY profiling float. Calculations from field deployments of a Seaglider and test tank trials of the openFloat show that salinity can be measured nearly identically by existing industry-grade and DIY AUVs. This method achieves salinity values to about ±0.20 PSU and is best used in dynamic coastal systems where salinity variation is high. This establishes a path forward for further development of the openFloat and a salinity calculation that could be used to extract more data from other buoyancy-driven devices.

**Acknowledgements**

This project thanks the University of Washington Ocean Technology Center for funding and facilities, the Student Seaglider Center for funding ship time, Sasha Seroy and Aadu Prakash for many hours of guidance and paper/code revisions, Trevor Harrison for early guidance on designing the VBE system, Imants Smidchens for CAD help and design ideas, Emily Barker for continual support, and Jenna Fernandez for supplying metric machine screws.

**References**

Babson, A. L., Kawase, M., & MacCready, P. (2006). Seasonal and interannual variability in the circulation of Puget Sound, Washington: a box model study. Atmosphere-Ocean, 44(1), 29-45. https://doi.org/10.3137/ao.440103.

Cox, R. A. (1963). The salinity problem. Progress in Oceanography, 1, 243–261. https://doi.org/10.1016/0079-6611(63)90006-5.

Eriksen, C. C., Osse, T. J., Light, R. D., Wen, T., Lehman, T. W., Sabin, P. L., Ballard, J. W., & Chiodi, A. M. (2001). SeaGlider: a long-range autonomous underwater vehicle for oceanographic research. IEEE Journal of Oceanic Engineering, 26(4), 424–436. https://doi.org/10.1109/48.972073.

Harrison, T. (2021). Buoyancy Controlled Float Swarms for Distributed Sensing in Coastal Waterways (Doctoral dissertation). Retrieved from Research Works Archive. (https://digital.lib.washington.edu/researchworks/handle/1773/47639). Seattle, WA: University of Washington.

Lauer, J. W., Klinger, P., O'Shea, S., & Lee, S.-Y. (2023). Development and validation of an open-source four-pole electrical conductivity, temperature, depth sensor for in situ water quality monitoring in an estuary. Environmental Monitoring and Assessment, 195(1), 221–221. https://doi.org/10.1007/s10661-022-10493-y.

Lukas, R., & Santiago-Mandujano, F. (2008). Interannual to Interdecadal Salinity Variations Observed Near Hawaii: Local and Remote Forcing by Surface Freshwater Fluxes. Oceanography, 21(1), 46–55. https://www.jstor.org/stable/24860154

Lyman, T. P., Elsmore, K., Gaylord, B., Byrnes, J. E. K., & Miller, L. P. (2020). Open Wave Height Logger: An open source pressure sensor data logger for wave measurement. Limnology and Oceanography, Methods, 18(7), 335–345. https://doi.org/10.1002/lom3.10370.

MacCready, P., McCabe, R. M., Siedlecki, S. A., Lorenz, M., Giddings, S. N., Bos, J., Albertson, S., Banas, N. S., & Garnier, S. (2021). Estuarine Circulation, Mixing, and Residence Times in the Salish Sea. Journal of Geophysical Research: Oceans, 126. https://doi:10.1029/2020jc016738.

McDougall, T. J., Jackett, D. R., Millero, F. J., Pawlowicz, R., & Barker, P. M. (2012). A global algorithm for estimating Absolute Salinity. Ocean Science, 8(6), 1123–1134. https://doi.org/10.5194/os-8-1123-2012.

Moore, S. K., Mantua, N. J., Newton, J. A., Kawase, M., Warner, M. J., & Kellogg, J. P. (2008). A descriptive analysis of temporal and spatial patterns of variability in Puget Sound oceanographic properties. Estuarine, Coastal and Shelf Science, 80(4), 545–554. https://doi.org/10.1016/j.ecss.2008.09.016.

Ovall, B. (2019). Density structure in the outflow region of Colvos Passage: Observational analysis and model comparison (Bachelor's thesis). Retrieved from Research Works Archive. (https://digital.lib.washington.edu/researchworks/bitstream/handle/1773/45629/ovallbridgetm_3724551_56873316_Ovall-1.SeniorThesis.FinalDraft.pdf?sequence=1&isAllowed=y). Seattle, WA: University of Washington.

Seim, H. E., & Gregg, M. C. (1997). The importance of aspiration and channel curvature in producing strong vertical mixing over a sill. Journal of Geophysical Research: Oceans, 102(C2), 3451–3472. https://doi.org/10.1029/96JC03415

Stammer, D., Martins, M. S., Köhler, J., & Köhl, A. (2021). How well do we know ocean salinity and its changes?. Progress in oceanography, 190, 102478. https://doi.org/10.1016/j.pocean.2020.102478.

Thaler, A., S.K. Sturdivant, R.Y. Neches, & J.J. Levenson. (2024). The OpenCTD: A low-cost, open-source CTD for collecting baseline oceanographic data in coastal waters. Oceanography, https://doi.org/10.5670/oceanog.2024.602.

Woody, C., Shih, E., Miller, J., Royer, T., Atkinson, L. P., & Moody, R. S. (2000). Measurements of Salinity in the Coastal Ocean: A Review of Requirements and Technologies. Marine Technology Society Journal, 34(2), 26–33. https://doi.org/10.4031/MTSJ.34.2.4.

548 **Appendix**

549 All data are made publically available here:

550 https://github.com/cflaim1123/openFloat_thesis/tree/main/data.

551 **Table 1** openFloat project budget.

| Category | Item | # | Price per | Total price |
|---|---|---|---|---|
| Electrical - general | perfboard (pack of 50) | 7 | $0.50 | $3.50 |
| | Misc wires | NA | NA | $15.00 |
| | Male header pins | NA | NA | $5.00 |
| | Female header pins | NA | NA | $5.00 |
| | Solder | NA | NA | $10.00 |
| | Resistors | NA | NA | $0.10 |
| | Misc GPS radio wires | NA | NA | $15.00 |
| Electrical - control | ESP32 feather huzzah v2 | 2 | $19.95 | $39.90 |
| | BLDC motor | 1 | $30.00 | $30.00 |
| | 5V, 5A voltage step-down regulator | 1 | $32.95 | $32.95 |
| | custom battery pack | 1 | $15.00 | $15.00 |
| Electrical - sensing | analog pressure sensor | 1 | $20.00 | $20.00 |
| | Thermistor | 1 | $2.00 | $2.00 |
| | adafruit data logger feather wing | 1 | $8.95 | $8.95 |
| | digital temperature sensor (pack of 5) | 1 | $10.00 | $10.00 |
| | BMP180 pressure sensor | 1 | $9.95 | $9.95 |
| | DHT22 humidity sensor | 1 | $9.95 | $9.95 |
| | TSL2591 lux sensor | 1 | $6.95 | $6.95 |
| | Adafruit 9-DOF absolute orientation IMU - BN055 | 1 | $35.00 | $35.00 |
| | Adafruit ultiamte GPS | 2 | $30.00 | $60.00 |
| | 915 mHz LoRa radio module | 2 | $20.00 | $40.00 |
| | Precision current meter | 1 | $10.00 | $10.00 |
| | GPS antenna | 1 | $20.00 | $20.00 |
| | Radio antenna | 2 | $10.00 | $20.00 |
| Mechanical | Low-pitch, high-precision ACME lead screw | 1 | $15.00 | $15.00 |
| | Misc O-ring | NA | NA | $10.00 |

| | | | | |
|---|---|---|---|---|
| | Misc PVC pipe for piston | 1 | $10.00 | $10.00 |
| | 4" PVC pipe | 1 | $20.00 | $20.00 |
| | 4" PVC endcaps | 2 | $10.00 | $20.00 |
| | metal cable glands | 5 | $10.00 | $50.00 |
| | Epoxy | 2 | $10.00 | $20.00 |
| | | | Total: | $529.25 |

552